SEASONAL INSTRUMENTATION OF SHRP PAVEMENTS - THE OHIO STATE UNIVERSITY

FINAL REPORT

THE OHIO STATE UNIVERSITY
2070 Neil Avenue, Columbus, OH 43210

September 1, 1998

Principal Investigator: William E. Wolfe
Co-Principal Investigators: Osama A. Abdulshafi
Tien H. Wu

Research Associates: Andrew C. Casto, Brett A. Dreger, Sharon F. Morland, Rodrigo Mendoza, Gokhan Inci, Xi-You Chen, Jennifer C. Myers

Prepared in Cooperation with the Ohio Department of Transportation and the U.S. Department of Transportation, Federal Highway Administration

1. Report No.	2. Government Accession No.	3. Recipient's Catalog No.
FHWA/OH-98/014		

4. Title and Subtitle	5. Report Date
SEASONAL INSTRUMENTATION OF SHRP PAVEMENTS - THE OHIO STATE UNIVERSITY	June 11, 1998
	6. Performing Organization Code
	8. Performing Organization Report No.
7. Author(s)	10. Work Unit No. (TRAIS)
William E. Wolfe, Osama Abdulshafi, T. H. Wu	
9. Performing Organization Name and Address	11. Contract or Grant No.
The Ohio State University Department of Civil Engineering Columbus, OH 43210	State Job No. 14586(0)
	13. Type of Report and Period Covered
	Final Report
12. Sponsoring Agency Name and Address	14. Sponsoring Agency Code
Ohio Department of Transportation 25 S. Front St. Columbus, OH 43215	

15. Supplementary Notes

Prepared in cooperation with the U.S. Department of Transportation, Federal Highway Administration

16. Abstract

Environmental instruments to measure temperature, soil moisture and frost depth were installed at five test sections of the SHRP pavement project on U.S. 23 north of Delaware, Ohio. At three of these locations tensiometers, which a designed to measure negative pore pressures, were added to the instrumentation package. The pore pressures as recorded by the tensiometers have increased from initially negative to positive values at each location and throughout the profile in the first year after installation of the instrument package was completed. At the same time, data collected from the moisture probes were showing a corresponding increase in soil moisture content.

Samples of an aggregate base and clayey subgrade material were collected at several locations on the DEL 23 project by ODOT. They were delivered to the OSU soil mechanics laboratory for classification and permeability determination. The aggregate base conformed to ODOT material specification Item 304. Measured permeability coefficients ranged between $2x10^{-2}$ and $2.9x10^{-2}$ cm/sec. The clayey material was classified as a low plasticity clay (AASHTO Classification A-6 to A-7-6) with permeability coefficients ranging between $1x10^{-6}$ and $4x10^{-8}$ cm/sec.

17. Key Words	18. Distribution Statement
Pavement Performance; Seasonal Monitoring; Tensiometers; Permeability Testing	No Restrictions. This document is available to the public through the National Technical Information Service, Springfield, Virginia 22161

19. Security Classif. (of this report)	20. Security Classif. (of this page)	21. No. of Pages	22. Price
Unclassified	Unclassified		

SEASONAL INSTRUMENTATION OF SHRP PAVEMENTS - THE OHIO STATE UNIVERSITY

FINAL REPORT

THE OHIO STATE UNIVERSITY
2070 Neil Avenue, Columbus, OH 43210

September 1, 1998

Principal Investigator: William E. Wolfe
Co-Principal Investigators: Osama A. Abdulshafi
Tien H. Wu

Research Associates: Andrew C. Casto, Brett A. Dreger, Sharon F. Morland, Rodrigo Mendoza, Gokhan Inci, Xi-You Chen, Jennifer C. Myers

Prepared in Cooperation with the Ohio Department of Transportation and the U.S. Department of Transportation, Federal Highway Administration

ACKNOWLEDGEMENTS

The Ohio Department of Transportation (ODOT) and the Federal Highway Administration (FHWA) supported this research.

The work presented in this report was part of a project to install and monitor seasonal instrumentation at five SHRP pavement sections. That effort was in turn part of a larger effort to install and monitor seasonal and structural performance instrumentation at 33 pavement test sections on US 23 in Delaware, Ohio. Many individuals participated in this research. Professor S. Sargand and his students and staff from Ohio University led the project team and contributed countless times to the success of this work. Interesting conversations with colleagues at Case Western Reserve University and the University of Toledo who were also installing seasonal instrumentation improved data collection methods. Help both on and off site from R. Green and B. Young from ODOT is appreciated.

TABLE OF CONTENTS

LIST OF TABLES

LIST OF FIGURES

1 INTRODUCTION

1.1 Background

The AASHTO Road Tests conducted in the late 1950's and early 1960's are still used in the design of highway pavements[1]. To better understand the mechanistic behavior of roadway pavements and so to improve performance, the Strategic Highway Research Program (SHRP) initiated a series of Specific Pavement Studies (SPS) designed to use modern instrumentation to assess pavement performance over extended periods of time.

As part of a national effort to acquire a large database of SPS information, the Ohio Department of Transportation (ODOT) constructed a series of test pavements on U.S. 23 in Delaware, Ohio. This program included 34 instrumented test sections in four different pavement configurations instrumented with environmental and dynamic devices to monitor seasonal and real-time effects of traffic and weather. Due to the scale of the study, ODOT distributed instrumentation installation and monitoring responsibilities among six Ohio universities (Ohio University, Ohio State University, Case Western Reserve University, University of Toledo, University of Cincinnati and Akron University).

The Ohio State team was responsible for calibration, installation and monitoring the environmental instrumentation at five sections comprising three of the four different SPS test pavements. The instruments installed measure soil moisture and temperature and frost depth profiles from the pavement surface down to a depth of about two meters. The guidelines describing the approved procedures for calibration, installation and monitoring are included in the Long Term Pavement Performance (LTPP) Seasonal Monitoring Program (SMP) manual[2]. In addition to this instrumentation, which was common to all environmental sites, OSU developed and constructed tensiometers to measure the matric suction in the subsurface soils and installed the devices at four locations. The environmental instruments were installed at the U.S. 23 Delaware site between August 1995 and August 1996. The proper operation of the devices was verified by collecting an initial set of data between September 6 and September 11, 1996. Monitoring continued for the remainder of the contract. The data from those readings and their implications are discussed.

1.2 Site Details

The location selected for the SPS experiments is on U.S. 23 north of Delaware, in Delaware County, Ohio. The project consisted of two southbound lanes for SPS-1 (flexible pavement) tests, and two northbound lanes for SPS-2 (rigid pavement). An SPS-8 (flexible and rigid light traffic) section was included on an on ramp to the southbound lanes since few vehicles use that entrance to the highway. An SPS-9 section (asphalt program field verification studies) was incorporated at the southern end of the site in the southbound lanes. In the section responsibilities as assigned by ODOT, Ohio

State University was given charge of sections J8 (SPS-1), J1, J11 and S4 (SPS-2) and SHRP (SPS-9). The relative positions of the OSU SPS test sections are given in Figure 1.1. Additional information about the three sites where tensiometers were installed is given in the general description of the research effort following a review of methods for evaluating shear strength and compressibility in unsaturated soils.

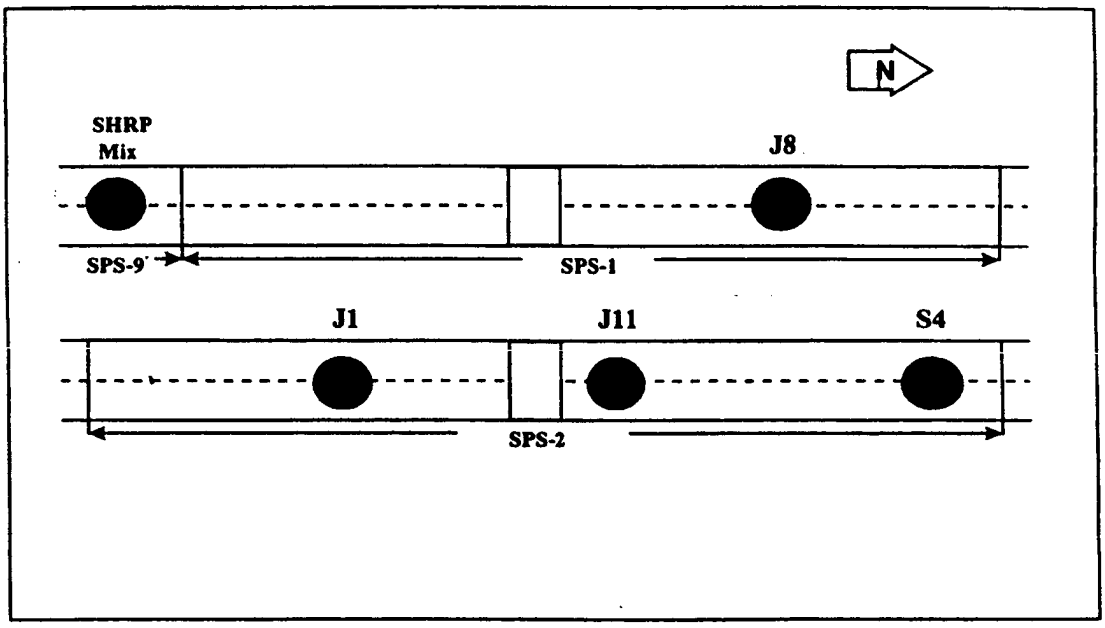

Figure 1.1 OSU Environmental Test Sections

2 RESEARCH OBJECTIVES

The present study was designed to provide more direct information on the state of stress in the subgrade materials at selected pavement sections of the US23 SHRP Project. The soil stress data collected was to complement the data collected from the SHRP instrumentation that was installed and monitored during the same time period. An extension of the original study objectives included a determination of the hydraulic conductivity of selected base and subgrade samples provided by ODOT.

3 DESCRIPTION OF THE RESEARCH

3.1 Literature Review

Soil strength and compressibility are typically determined in the laboratory using fully saturated samples. The saturated condition is specified because it usually represents a realistic worst case for design purposes. However, when material types and drainage conditions can be controlled, complete saturation may not be consistent with the actual in-situ conditions. In these cases, because unsaturated soils are not adequately described by classical soil mechanics, the assumption of 100% saturation can lead to potentially large discrepancies between in-situ properties and commonly used design parameters. A brief review of saturated soil mechanics and Fredlund and Rahardjo's[5] methods for unsaturated soil mechanics as they relate to strength and compressibility is presented. In addition, the rationale for selection of the probes used to measure matric suction is presented.

3.1.1 Saturated Soil Mechanics

The state of stress at a point in a soil mass must be known if the mechanical behavior of the soil is to be accurately characterized. The number of state variables required to adequately describe the stress state in a soil depends on the number of material phases actually present[5]. When dealing with a saturated soil, i.e. a two phase material, the one stress state variable used to describe soil response is the effective stress. The effective stress is defined as the difference between the total (applied) stress and the pore-water pressure[5]

$$\sigma' = \sigma - u_w \tag{3.1}$$

where:

σ = total normal stress
u_w = pore-water pressure
σ' = effective normal stress

In saturated soils, one stress state variable, σ', is required to describe the mechanical behavior. The use of the effective stress concept to describe soil behavior has been long established and experimentally verified.[6,7] The shear strength of a saturated soil is typically described by the Mohr-Coulomb failure criterion using the effective stress concept:

$$\tau_f = c' + (\sigma_f - u_w)_f \tan\phi' \tag{3.2}$$

where:

τ_f = shear stress on the failure plane at failure
c' = effective cohesion

$(\sigma_f - u_w)$ = effective normal stress on the failure plane at failure
ϕ' = effective angle of internal friction.[8]

Equation 3.2 describes a line in stress space.

The constitutive relationship between void ratio and effective stress describes how the soil structure will react to changes in effective stress. This relationship can be represented by the following equation:

$$de = a_v d(\sigma - u_w) \tag{3.3}$$

where:

de = incremental void ratio
a_v = coefficient of compressibility
$d(\sigma - u_w)$ = incremental change in effective stress[9]

3.1.2 Unsaturated Soil Mechanics

3.1.2a Stress State Variables

While saturated soils can be described as having two constituent phases, water and soil solids, unsaturated soils consist of four distinct phases, the water and soil solids of the saturated case plus air and the contractile skin. The contractile skin, which is the air-water interface, is treated as a separate phase due to its distinctive properties. Its density is less than that of the water phase and it has the ability to exert a tensile pull on the soil particles. When the air phase is continuous the contractile skin acts like an elastic membrane interweaving throughout the soil structure. When performing a stress analysis it is important to recognize the contractile skin as a separate, individual phase.

The stress state variables for unsaturated soils are extracted from the total force equilibrium equations from the air phase, the water phase and contractile skin. These variables are:

$$(\sigma - u_a) \quad \text{and} \quad (u_a - u_w)$$

where:

u_a = the pore-air pressure.[10]
$(\sigma - u_a)$ = the net normal stress
$(u_a - u_w)$ = the matric suction.

3.1.2b Shear Strength

The shear stress at failure can be determined from the aforementioned stress state variables using the following equation:

$$\tau_f = c' + (\sigma_f - u_a)_f \tan\phi' + (u_a - u_w)_f \tan\phi^b \quad (3.4)$$

where:

c' = effective cohesion (intercept of the extended Mohr-Coulomb failure envelope when the net normal stress and matric suction are zero)

$(\sigma_f - u_a)_f$ = net normal stress state on the failure plane at failure

$\tan\phi'$ = angle of internal friction associated with the net normal stress state variable

$(u_a - u_w)_f$ = matric suction on the failure plane at failure

$\tan\phi^b$ = angle indicating the rate of increase in shear strength relative to the matric suction. [11]

Inspection of Eq. 3.4 shows that the shear strength for an unsaturated soil is related to the strength of the saturated soil. As the soil approaches saturation, the value of the porewater pressure, u_w, approaches that of the pore-air pressure, u_a , and the matric suction, represented by (u_a-u_w), goes to zero.

3.1.2c Extended Mohr-Coulomb Failure Envelope

The failure envelope for a saturated soil is described using a two dimensional plot. For unsaturated soils the failure envelope may be best described by employing a three dimensional plot in which matric suction is incorporated as the third dimension. This representation of strength is termed the extended Mohr-Coulomb failure envelope. The failure criterion is extended to include suction effects while degenerating to the expression for saturated soils when the matric suction goes to zero. The Mohr circles for an unsaturated soil are plotted with respect to the net normal stress axis in the same way the stress circles for saturated soils were plotted with respect to the effective stress axis. The surface tangent to the circles at failure is the extended Mohr-Coulomb failure envelope[5]. Figure 3.1 is an illustration of the Mohr-Coulomb failure criterion, as it would be used for unsaturated soils.

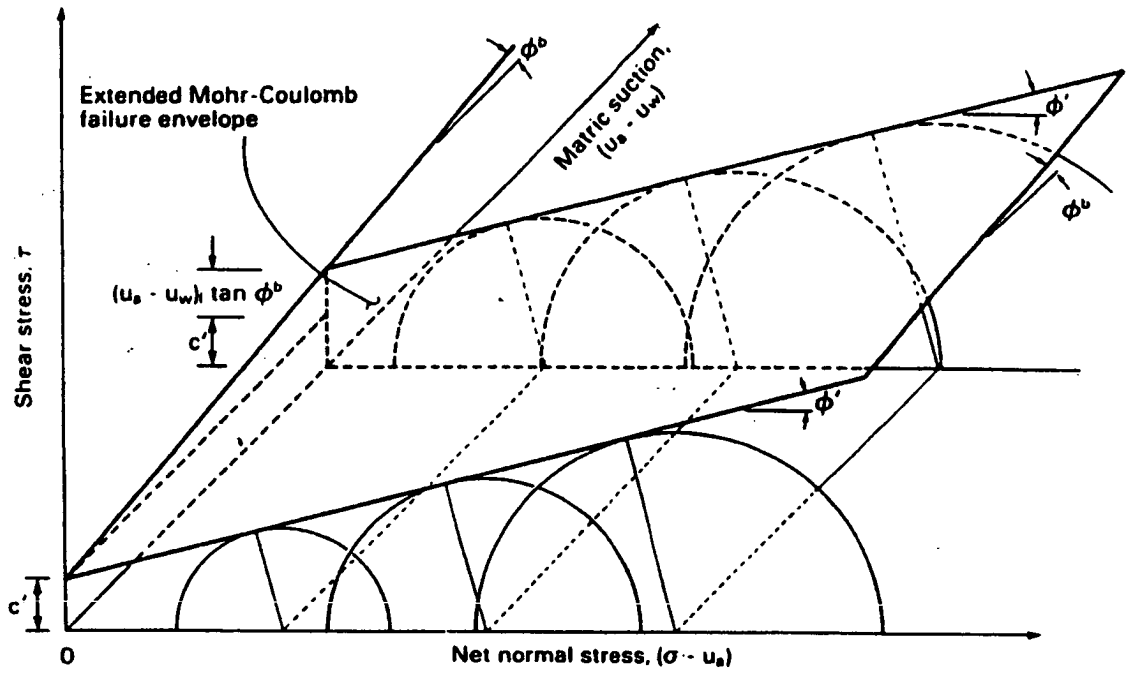

Figure 3.1 Mohr-Coulomb Failure Criterion for an Unsaturated Soil [5]

The parameters ϕ', ϕ^b and c′ are used to relate the shear stress at failure to the stress state variables, $(\sigma - u_a)$ and $(u_a - u_w)$. Strength changes due to an increase in net normal stress are described by the parameter ϕ', whereas changes in strength due to changes in matric suction are described by ϕ^b. The parameters, ϕ', ϕ^b and c′ are determined experimentally, in the same way the effective friction angle and effective cohesion are measured for a saturated soil, i.e., by controlling the pore-air pressure, pore-water pressure and normal stress on a test specimen for a series of strength tests.

3.1.2d Compressibility

The relationship between void ratio and the stress state variables describes how the soil structure reacts to changes in net normal stress and matric suction. It is an extension of the expression for saturated soil and is given as:

$$de = a_t d(\sigma_{mean} - u_a) + a_m d(u_a - u_w) \tag{3.5}$$

where:

a_t = coefficient of compressibility with respect to a change in net normal stress

a_m = coefficient of compressibility with respect to a change in matric suction [9]

The above equation can be visualized as a three-dimensional plot. If the matric suction is zero, an increase in net normal stress results in a decrease in void ratio. If the matric suction is not zero, the void ratio decreases as the net normal stress increases, but the amount of the decrease is less than for a soil with zero or a smaller initial value of matric suction. Therefore, the soil with a large matric suction appears less compressible under the same change in net normal stress.

3.2 Selection of Instruments to Measure Water Pressure in Unsaturated Soil

Accurate measurement of porewater pressure in an unsaturated medium requires a sensing unit that is impervious to air while allowing water to flow across the soil/sensor boundary. Two devices that have been used for this purpose were considered for the Del 23 application. The two devices are the thermal conductivity sensor, and the tensiometer. The thermal conductivity sensor is enclosed in an initially saturated porous ceramic block. Water in the block interacts with the pore water and comes to equilibrium. The thermal conductivity of the cup changes as the moisture content of the block changes. The sensor must be calibrated for a given soil to relate matric suction to thermal conductivity. The range of negative pressures that can be measured with a thermal conductivity sensor is large (greater than with a tensiometer) but thermal conductivity is an indirect way to measure matric suction. Furthermore, these devices are very fragile and, even when handled with great caution during controlled experiments in a laboratory, many crack or crumble during calibration and installation.[5] The electronics seem to be prone to difficulties as well, since failures related to the deterioration of the electronics within the ceramic have been reported.[5] Given that the thermal conductivity sensors have a history of being fragile and those that do work only make an indirect measurement of matric suction, tensiometers were chosen for this research. A tensiometer consists of a porous ceramic cup, a small diameter tube and a pressure measuring device. The porous ceramic cup is placed in the soil at the location where the water pressure measurement is to be made. The small bore tube connects the cup to the pressure sensing device. The porous cup is saturated and the entire system is filled with water. When the water in the cup is in contact with the porewater and equilibrium has been established, the porewater and the water in the tube must be at the same pressure. The pressure in the cup can be measured using a gage referenced to a vacuum rather than atmospheric pressure. For the system to work properly, the tube and cup must be sealed to prevent air from entering the system at any location. The pore space of the soil, which is in general not saturated, contains air at atmospheric pressure, while the porewater pressure in the unsaturated soil will be at some value less than atmospheric. With this pressure difference, poreair would flow into the tensiometer and water would flow out, making a correct water pressure reading impossible. By using a saturated ceramic cup with pores small enough to inhibit the flow of air, negative water pressures can be sustained and measured. The air entry value, which is defined as the pressure difference required to move an air bubble through a saturated ceramic pore, can be calculated by:

$$P = 30 \times \frac{\sigma}{D} \tag{3.6}$$

where:

P = The air entry value expressed in millimeters of mercury.
D = Pore diameter in microns.
σ = Surface tension for water measured in dynes/cm.[3]

For example, the diameter of the pores in a ceramic with an air entry value of 1 bar (750 mm of mercury) would be:

$$D = 30 \times \frac{72}{750} = 2.9 \text{ microns} \tag{3.7}$$

As long as the ceramic's air entry value is greater than the expected soil suction the system will retain water and operate properly.

3.3 Sensor Construction

In general, commercially available tensiometers are not well suited for determining soil suction under a roadway, because they are straight tubes that extend vertically from the tip. Under a roadway the porous tip must be located beneath the pavement but the pressure sensing end must be accessible and so emerge several feet away. To meet the requirements of the project, the tensiometers we used were constructed at OSU. The OSU tensiometers were fabricated using copper tubing and fittings, porous ceramic cups and epoxy. The supplies used in the construction were:

- Model 652 Round Bottom Straight Wall Cups, air entry value of 1 bar, standard flow. Part # 652X08-B1M1 Soilmoisture Equipment Corp.[4]
- 12.7 mm (½ inch) hard copper tubing.
- 15.9 mm soft copper tubing.
- Copper fittings; couplings, tees, adapters, and reducers.
- 3M #2158 B/A Two Part Epoxy

The first step in construction was to solder all copper tubing and fittings together. Tensiometers were installed at three SPS sections and at the site weather station. At each SPS location, three tensiometers were installed, one at the top of the subgrade, a second 39.5 cm (12 inches) into the subgrade, and a third 61 cm (24 inches) into the subgrade. At the weather station a tensiometer was placed 39.5 cm and another 61cm under the soil surface.

The tensiometers for the SPS sections (SPS-9 SHRP, SPS-2 J11, SPS-2 S4) were initially constructed to extend two feet past the shoulder making the total tube length equal to six meters. In this section of each tensiometer we used the hard copper tubing.

The remainder of the distance to the final location off the shoulder was completed after grading the drainage ditches with the flexible tubing. The tensiometers at the weather station were constructed using hard copper tubing. The pressure sensing end of each tensiometer included a 20 cm standpipe for filling the system with water, a tee, and the female adapter for connecting the pressure sensing device and sealing the standpipe. Each porous tip was epoxied into a reducer. That assembly was then soldered onto the copper tubing. A heating cable was fastened to the tubing just above the ceramic tip and wrapped around the tubing from about 2 cm above the tip to about 20 cm above the tip. The heating cables were spliced onto 16 meters of 14-2 G.W. UFB wire extending the length of the probes back to the pull-boxes. After the heating cables were made secure, the tensiometers were ready for calibration and installation.

3.4 Transducer Calibration

The device used for sensing pressure in the tensiometer was a pressure transducer capable of measuring absolute water pressures from 0 to 350 kN/m^2. In order to correctly relate the transducer's output voltage to a suction value each transducer was calibrated against a certified vacuum gage. Readings of the transducer output were taken beginning at atmospheric pressure (0 bar) in 10 kN/m^2 (0.10 bar) increments up to 90 kN/m^2 (0.9 bar) and returning to 0. Then from 0 the pressure was decreased and readings were taken down to –90 kN/m^2 and then back to 0. This total pressure circuit was completed twice for each transducer. The voltages were recorded for the known values of pressure and vacuum, and a relationship between output voltage and system pressure was established.

3.5 Tensiometer Signal Conditioning

A multi-channel power supply and signal conditioner manufactured by Sensotec was used to supply the constant DC voltage excitation signal required by the transducers. The signal conditioner was also used to amplify the low level output signal from the Sensotec Model A-5 pressure transducer. The output from the amplifier was connected to a multimeter for recording.

3.6 Tensiometer Installation

Installation of the instrumentation at the Ohio State University SPS sections occurred between August 1995 and August 1996. Ten TDR's for moisture content one MRC thermistor probe for temperature and one CRREL resistivity probe to measure frost depth were all installed at each section. Three tensiometers for negative pore water measurements were installed at each of three pavement sections. An additional set of two tensiometers was installed at the weather station. This section discusses the procedure for installing the tensiometers. The actual in-place elevations and as well as the

measurements of each section acquired during installation are presented in the sections following the basic procedure.

3.6.1 Installation Procedure

The tensiometers were installed at the same time the standard environmental instrumentation was placed in the test sections. The installation procedure followed for each instrument was similar. However, since each section consisted of a different type and thickness of surface and base materials, the actual location of the instruments varied from section to section. Installation of each instrument package typically took several hours to complete and in some cases more than a day was required. Installation of the tensiometers proceeded as follows:

1. The location for the tensiometer package, consisting of three tensiometers, was chosen to be three feet from the SMP instruments to eliminate any potential for interference from the AC currents used on the tensiometer heating cables. The position was marked and the base removed down to the subgrade over a 0.3-meter diameter area. A trench was dug from the prepared area to the outside of the lane extending 0.6 meters past the edge of the shoulder. The tensiometers had to be extended to reach past the edge of the shoulder but not too far so they would not interfere with the placement of edge drains.
2. Using a hand auger a hole 4 cm in diameter was made in the subgrade down to 1 cm above the planned location for the tensiometer. A thin walled insertion tube, which was connected to the end of a 1.2 meter section of steel pipe, was used to remove a plug of soil at the bottom of the auger hole. The plug removed was slightly smaller in diameter than the outside diameter of the ceramic tip on the tensiometer, so that a good contact between the tip and the soil could be insured. The tensiometer was positioned in the hole and pressed firmly into place. The top tensiometer was placed horizontally just above the subgrade. After placing all three tensiometers at a single location, the trench was backfilled and the soil tamped. The tensiometer tubing stayed at this state until the paving was complete.
3. Once the sections were paved and the side drains were final graded, the installation was completed. The copper tubing was located using the wire for the heating cables, which was kept above ground at the end of the tubing. A trench was made from this location to the pull-boxes using a walk behind trencher. The tubing was then soldered to the existing hard tubing and extended to the pull-boxes.
4. The final step in the installation of the tensiometers was the fitting of the tubing and the wires with the proper connections. A tee made with a fill tube and a connection for the pressure transducer was attached to the end of the tubing in the pull-box. The wires for the heating cables were cut, leaving approximately one meter in the boxes. Each end was then fitted with a receptacle plug.

Instrumentation Section	SHRP Designation	Location (station)
SPS-9 SHRP	390904	301+83 to 302+17
SPS-2 J11	390211	373+95 to 374+20
SPS-2 S4	390263	421+06 to 421+31

Table 3.1 Station Locations for SPS Sections

3.6.1a Section SPS-9 SHRP

The SMP instrument installation for SPS-9 SHRP (Section Identification 390904), excluding trenching, was completed on August 15, 1995. The section limits for SPS-9 SHRP are given in Table 3.1. The composition of the surface and base is given in Table 3.2. The initial installation of the three tensiometers was performed on August 15, 1995, before the section was paved. Trenching and laying the cables from the tensiometer to the pull-box were completed on June 4, 1996. The tubing and wires for the tensiometers were extended to the same pull-box as the SMP instruments on June 13, 1996.

3.6.1b Section SPS-2 J11

The SMP instrument installation for SPS-2 J11 (Section Identification 390211), excluding trenching, was completed on September 13, 1995. The section limits are given in Table 3.1. The composition of the surface and base is given in Table 3.2. The initial installation of the tensiometers was accomplished on September 15, 1995, before the paving was completed. Trenching so the cables could be extended to the pull-box was completed on June 4, 1996. The pull box housing the cables from the SMP devices was not used for the tensiometers because the location of the pull box was not ideal for routing the tubing. The tubing and wires for the tensiometers were extended on August 5, 1996 to a metal pull-box constructed in the OSU CE Department machine shop.

3.6.1c Section SPS-2 S4

The SMP instrument installation for SPS-2 S4 (Section Identification 390263), excluding trenching, was completed on September 28, 1995. The section limits are given in Table 3.1. Composition of the surface and base materials is given in Table 3.2. The initial installation before paving was completed on October 10, 1995. Trenching of the cables to the pull-box was completed on June 4, 1996. As in the previous section, the location of the SMP pull-box was not well suited for routing the tubing, so the tubing and wires for the tensiometers at this section were extended to a second pull-box on August 6, 1996.

SECTION	SURFACE LAYER	STRENGTH	BASE TYPE AND THICKNESS	DRAIN
SPS-2 J11	11" Portland Cement Concrete (PCC)	ODOT	4" Permeable Asphalt Treated Base (PATB) / 4" Dense Graded Aggregate Base (DGAB)	YES
SPS-2 S4	11" PCC	ODOT	6" DGAB	YES
SPS-9 SHRP	4" Asphalt Cement Concrete (ACC)	na	12" Asphalt Treated Base (ATB) / 4" PATB / 6" DGAB	YES

Table 3.2 Surface and Base Materials at the OSU Sections

The tensiometers that were installed at the three SMP sections were placed at depths of 0, 30.5 and 61 cm (0, 12 and 24 inches) below the base. At the weather station the surface tensiometer was eliminated so that comparisons could be made between the tensiometers not covered by pavement, and those located at the SMP sections to determine the effects due to the pavement and resulting loads.

3.7 Laboratory Tests

Samples of granular and cohesive material were taken at several locations from the base and subgrade at the DEL 23 project by ODOT and delivered to the OSU soil mechanics laboratory. The samples received consisted of eighteen bags of aggregate base (item 304), four bags of a clayey material, and twelve Shelby tubes of a clayey material. This chapter describes the laboratory tests performed to characterize and classify these materials.

3.7.1 Granular material

3.7.1a Classification Tests

Sieve analyses were performed on the samples and the results compared to the material specifications stated by the Ohio Department of Transportation. The samples were found to be non-plastic and the grain size distribution met the requirements for Item 304, aggregate base. The material was classified as GW, a well graded gravel with little fines under the Unified Classification System and A-1-a under the AASHTO Classification System. The compaction characteristics of the aggregate were investigated following ASTM Standard Designation D 698 – 91, procedure C (Test method for laboratory compaction characteristics of soil using standard effort). The samples for the

permeability tests were prepared near the optimum moisture content to reproduce the conditions of the material in the field.

3.7.1b Permeability Tests

ASTM Standard Designation D 2434 - 68 (Test method for permeability of granular soils. Constant head) was used to determine the coefficient of permeability of the granular material. The tests were performed in 10 cm I.D. compaction molds as opposed to the 15 cm I.D. cylinder suggested. This modification reduced the effects of sample disturbance by allowing the permeability tests to be conducted directly in the compaction mold. In the following section, the results of the tests conducted are presented.

3.7.2 Fine Grained Material

3.7.2a Classification Tests

Plastic and liquid limit determinations were conducted on material that had been broken down as much as practically possible without crushing any granular particles present. Both samples were classified as CL, inorganic clays of low to medium plasticity, under the Unified Classification System and as A-6 (Sample 390204) and A-7-6 (Sample 390901) under the AASHTO Classification System. The compaction characteristics of the material were investigated by following ASTM, D698 - 91 (Test method for laboratory compaction characteristics of soil using standard effort), Procedure A.

3.7.2b Permeability Tests on Disturbed Cohesive Soil Samples.

Using the compaction data, each specimen for the permeability test was prepared at the optimum moisture content. Saturation of the samples was achieved by subjecting the samples to a backpressure of 138 kN/m^2, and a small hydraulic gradient for a period of 24 hours. ASTM Standard Designation D5084 -90 was used as the basis for the permeability tests. A falling head system and the 10 cm compaction mold permeameter were used in the determination of the coefficient of permeability for the two samples.

3.7.2c Permeability Tests on Undisturbed Cohesive Soil Samples.

ASTM Standard Designation D 5084 - 90 (Test method for measurement of hydraulic conductivity of saturated porous materials using flexible wall permeameter) was followed for the determination of the coefficient of permeability of the undisturbed cohesive samples collected at different locations. The tubes were split lengthwise to avoid compression or any type of disturbance that might have been caused by the extrusion device. All the intact samples were visually identified as stiff to very stiff brown clay with little fine gravel except for samples 390260 and 390902 in which traces of coarse gravel were found, and sample 390810 which was a silty clay. Each test specimen was prepared from a representative portion of one of the nine Shelby tubes received. The samples were tested after trimming the ends to make them plane and perpendicular to the longitudinal axis. As stated by the standard, a height to diameter ratio of one was followed to obtain the size of the test specimens.

A falling head hydraulic system was used to saturate each sample and then to perform the permeability test. The permeameter cell was filled with tap water while deaired water was used as the permeant liquid to facilitate saturation. To saturate the specimens, a backpressure was applied in increments of 70 kN/m^2. Before beginning each permeability test, a cell pressure of approximately 280 kN/m^2 was applied for a period of 48 hours. To maintain a positive effective stress approximately equal in magnitude to the in-situ stress under the roadway, a constant cell pressure 10 to 20 kN/m^2 greater than the influent and effluent pressures was applied. A hydraulic gradient of 20 was maintained during the tests.

4 RESULTS

4.1 Tensiometer Data

Figures 4.1 through 4.8 present the water pressure data obtained from the four tensiometer stations over the period of one year, beginning shortly after construction of the test sections was completed in Fall, 1996. In Figures 4.1 through 4.4 the pressure as a function of location in the subsurface profile is plotted. The vertical line at the centerline of each figure is zero pore pressure, which is the value that would be expected in a free draining granular material above the water table. The dashed line represents the value of the pore water pressure as a function of depth for the case of a static water table located at the base of the pavement.

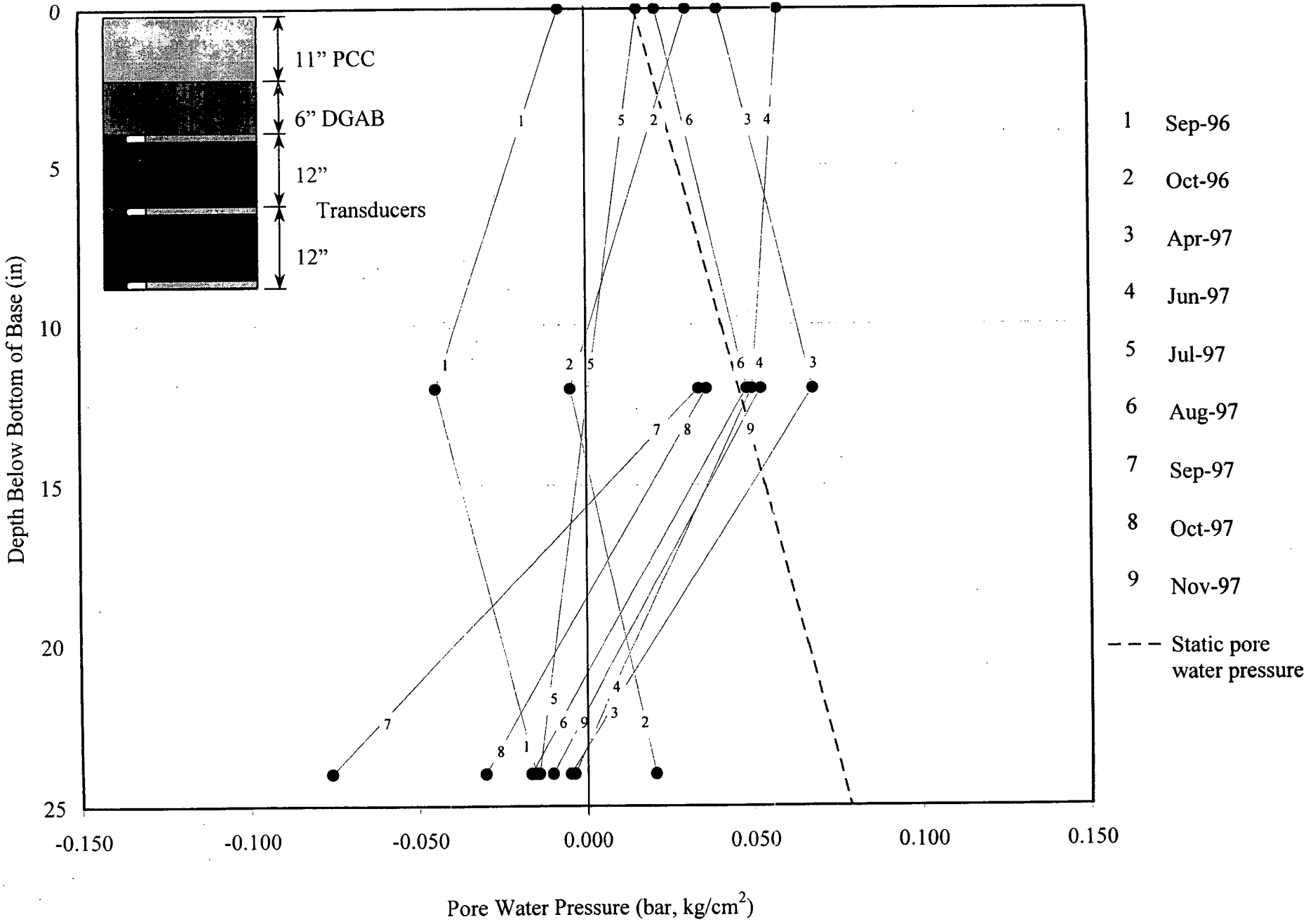

Figure 4.1. Pore Water Pressure Measurements at SPS-2 S-4. Section 390263.

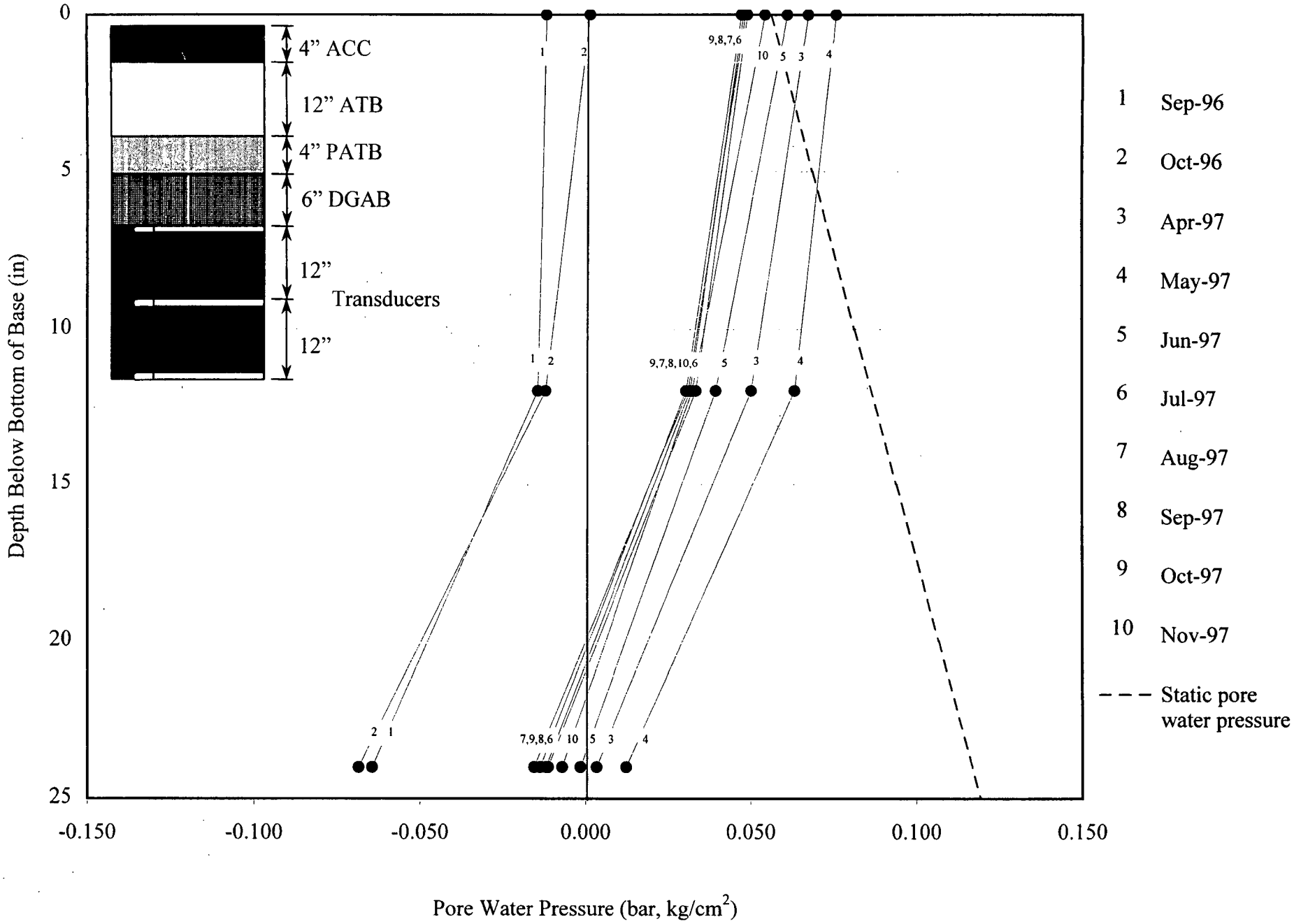

Figure 4.2. Pore Water Pressure Measurements at SPS-9 SHRP. Section 390904.

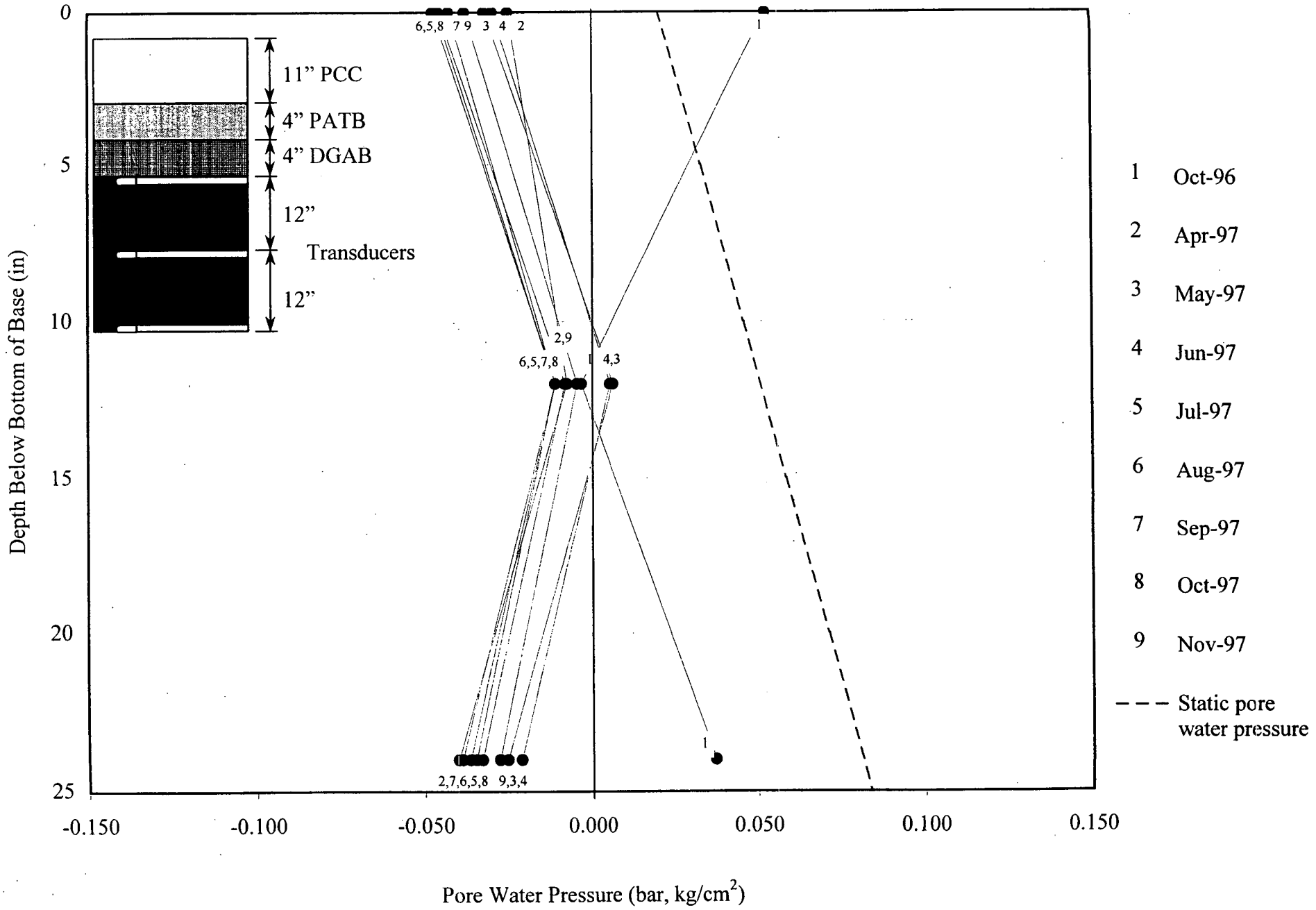

Figure 4.3. Pore Water Pressure Measurements at SPS-2 J-11. Section 390211.

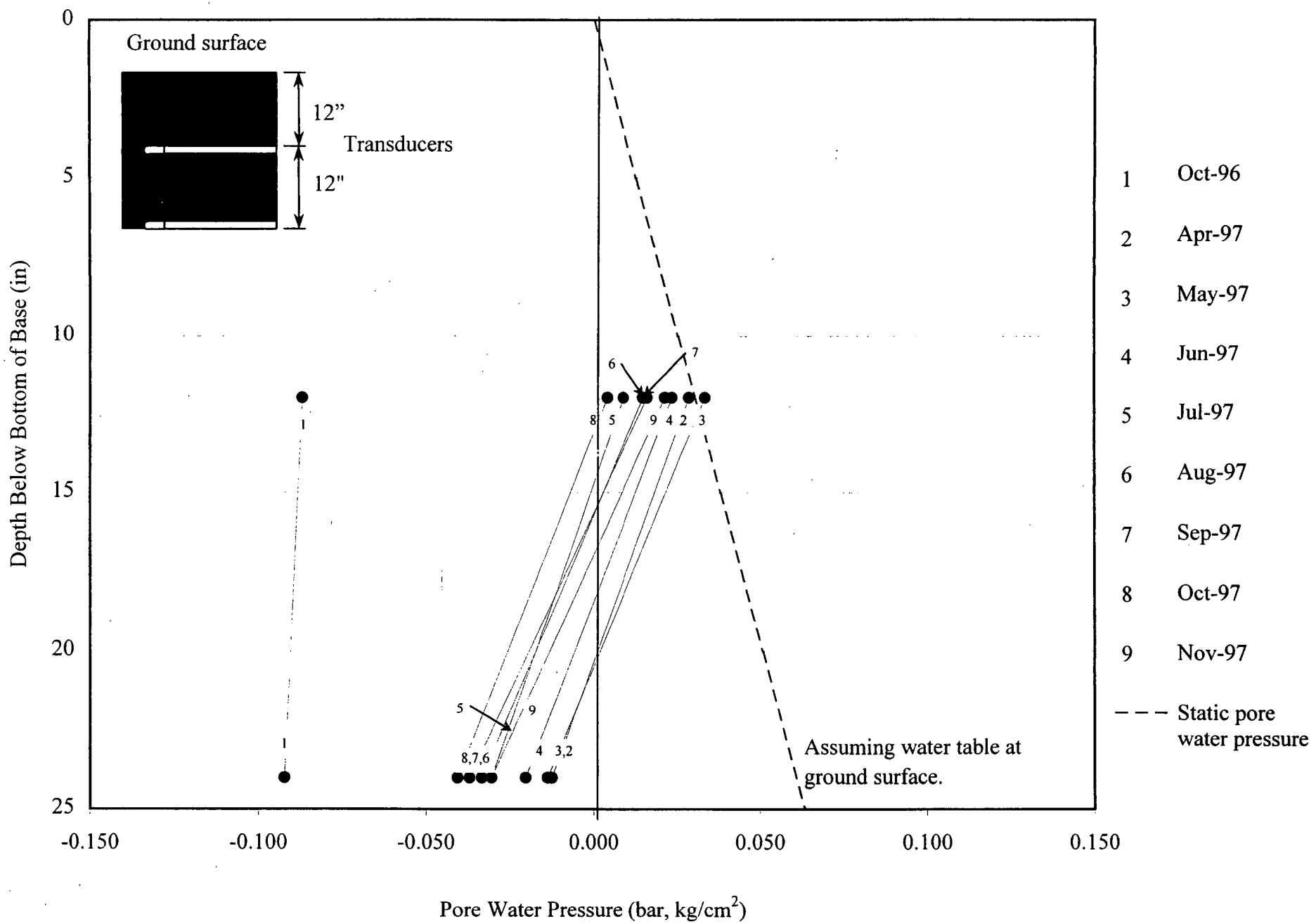

Figure 4.4. Pore Water Pressure Measurements at Weather Station.

In two sections the instrumentation was calibrated and installed in September 1996 (SPS-2 S-4 and SPS-9 SHRP). Both these sections show slightly negative pore pressures at all three elevations. The tensiometers at the remaining two stations (SPS-2 J-11 and the weather station) were first monitored in October 1996. Negative pore pressures were recorded at the weather station and at the mid-height location of SPS-2 J11. At the other two elevations (the bottom of the base course and a depth of 61 cm below the base) pore pressures were already positive at the time of tensiometer installation. Figures 4.5 through 4.8 present the same water pressure data but the changes with time are more apparent. The October readings at the SHRP section show little change in the pore pressures from the values recorded in September while at SPS-2 S4 the increase in pore pressure was approximately 4kN/m^2 (0.6 psi). Because the pressure transducers were removed during the winter to protect them from damage due to freezing temperatures, the next measurements were taken in April 1997. Three of the four locations showed a significant increase in the pore pressures over the winter months. Only SPS-2 J11, which had been read once in October, registered a decrease in pore pressure when first read again in April 1997. The positive pore pressures continued to increase through the spring followed by a decrease in pressure during the summer and fall months.

A comparison of the water content data, as recorded by the TDR's, which were located approximately one meter from the tensiometers, shows increases in water content corresponding to the increases in pore pressures. A comparison of the tensiometer data with the readings obtained from the TDR's is shown in Figures 4.9 through 4.11. Seasonal changes in water content are apparent, and although additional readings are necessary before an equilibrium water content and pore pressure can be clearly established, the trend is toward greater moisture contents and larger porewater pressures. These data strongly suggest that water is being drawn up into the profile from depth. The initial negative pore water pressures are a strong indication that the base and subgrade should not be considered to be free draining.

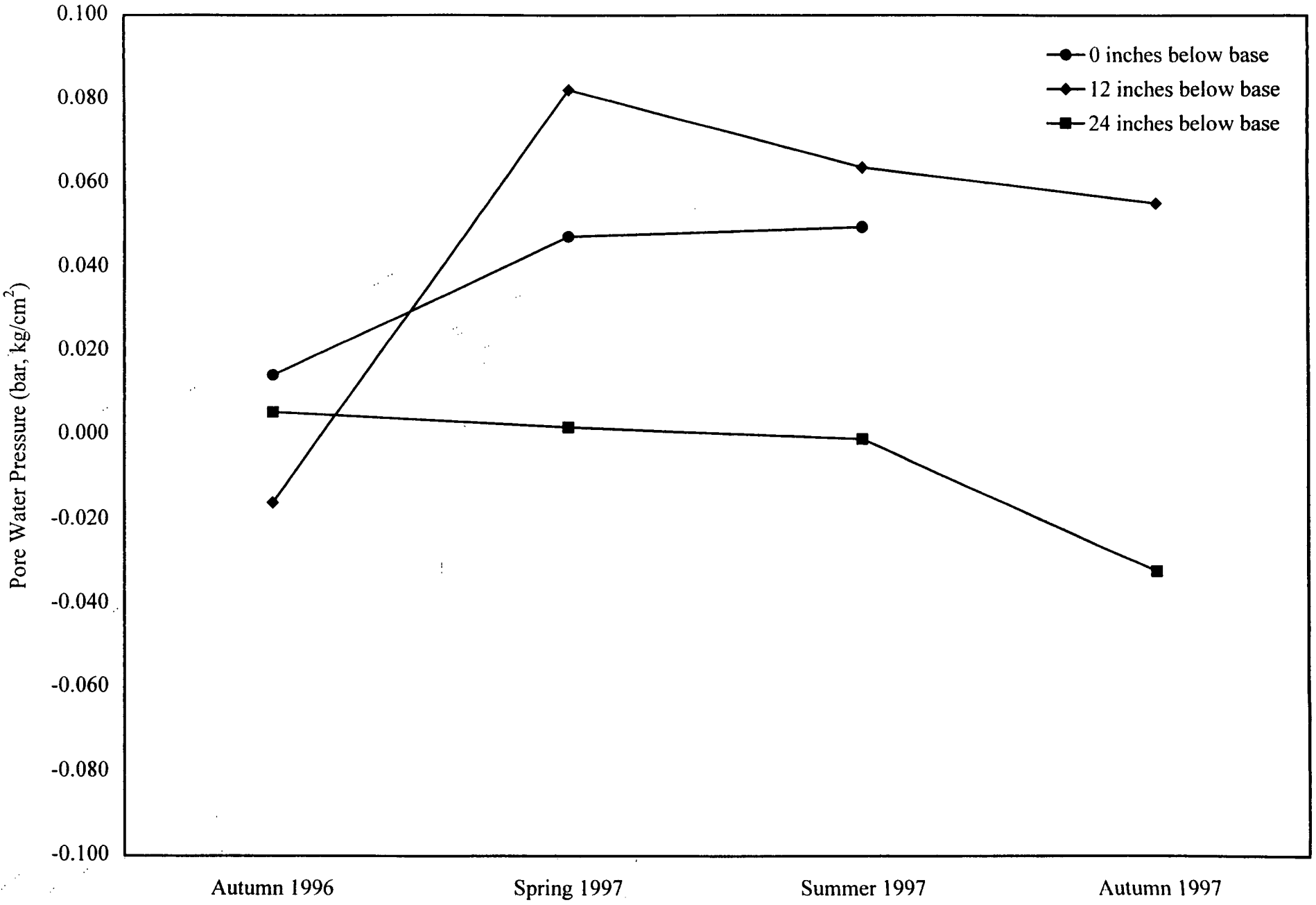

Figure 4.5. Pore Water Pressure Measurements vs Time at SPS-2 S-4. Section 390263.

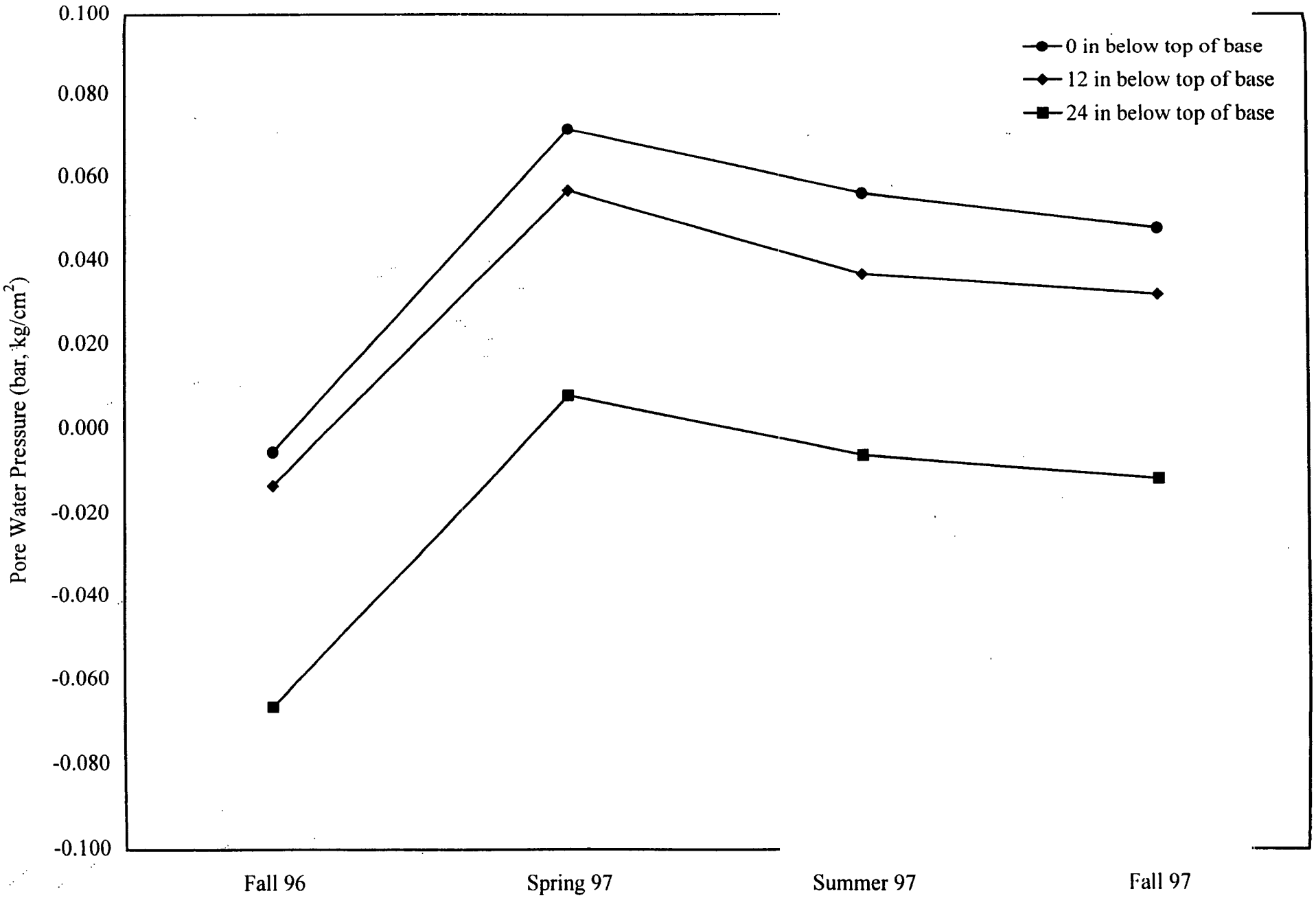

Figure 4.6. Pore Water Pressure Measurements vs Time at SPS-9 SHRP. Section 390904.

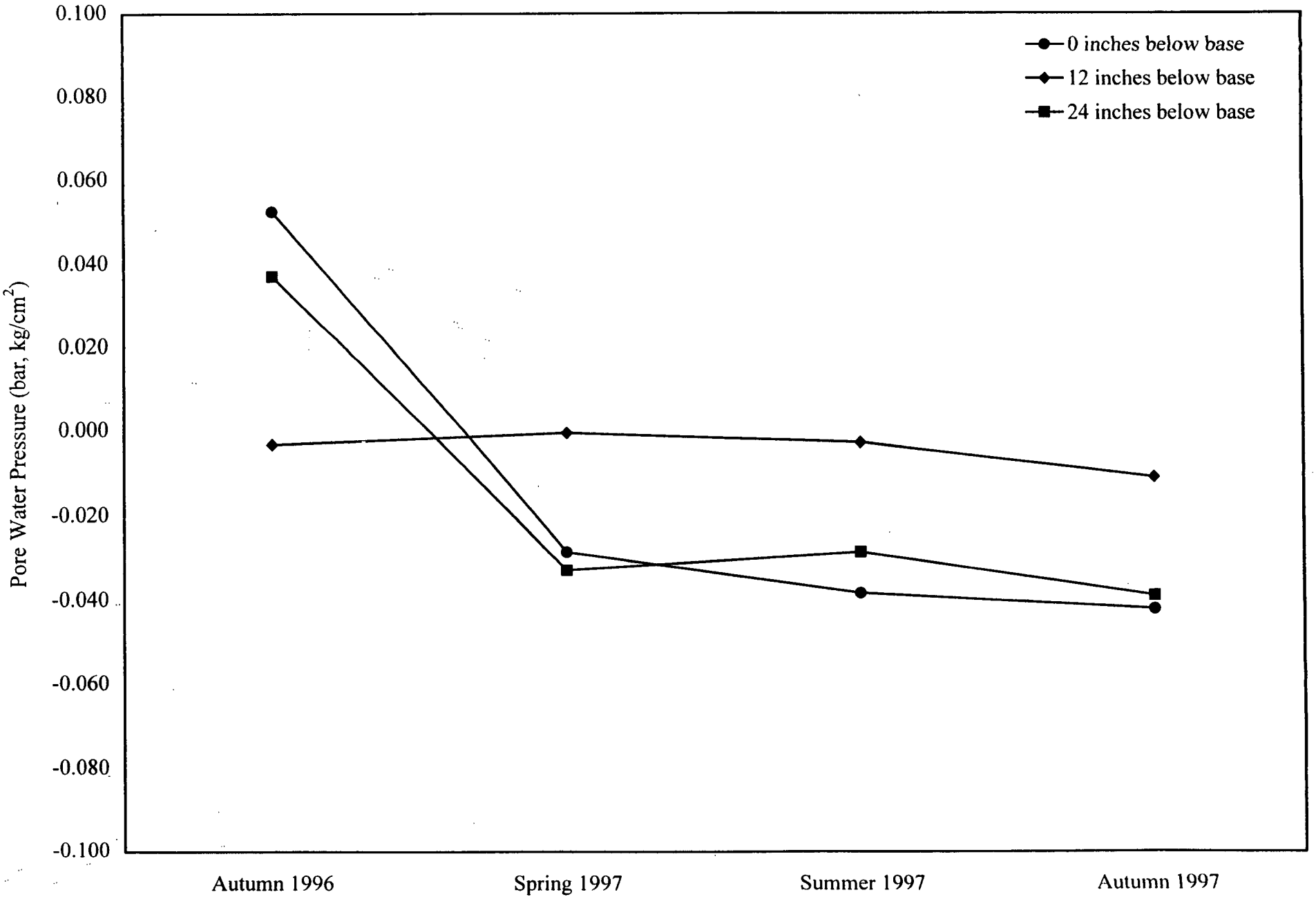

Figure 4.7. Pore Water Pressure Measurements vs Time at SPS-2 J-11. Section 390211.

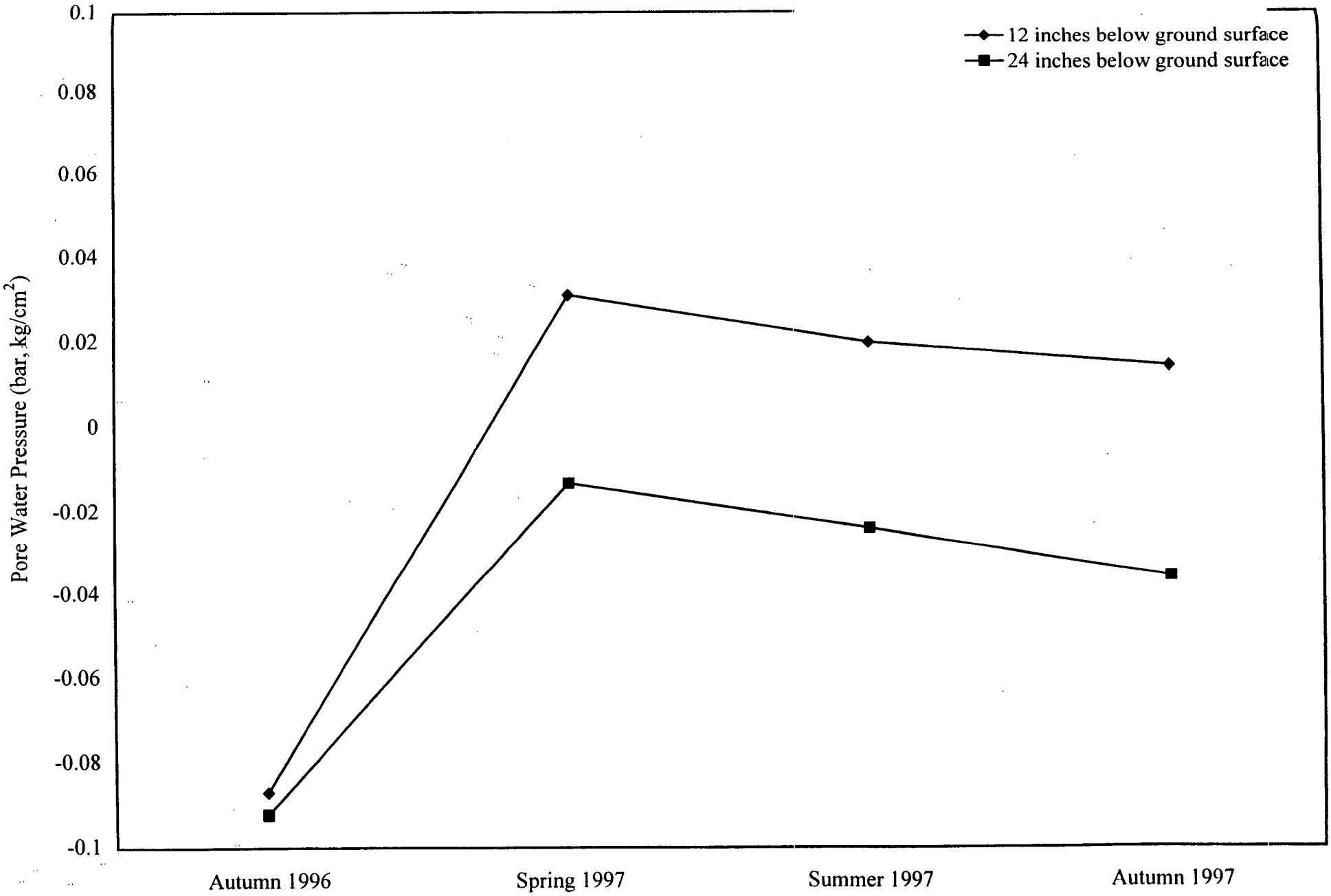

Figure 4.8. Pore Water Pressure Measurements vs Time at Weather Station.

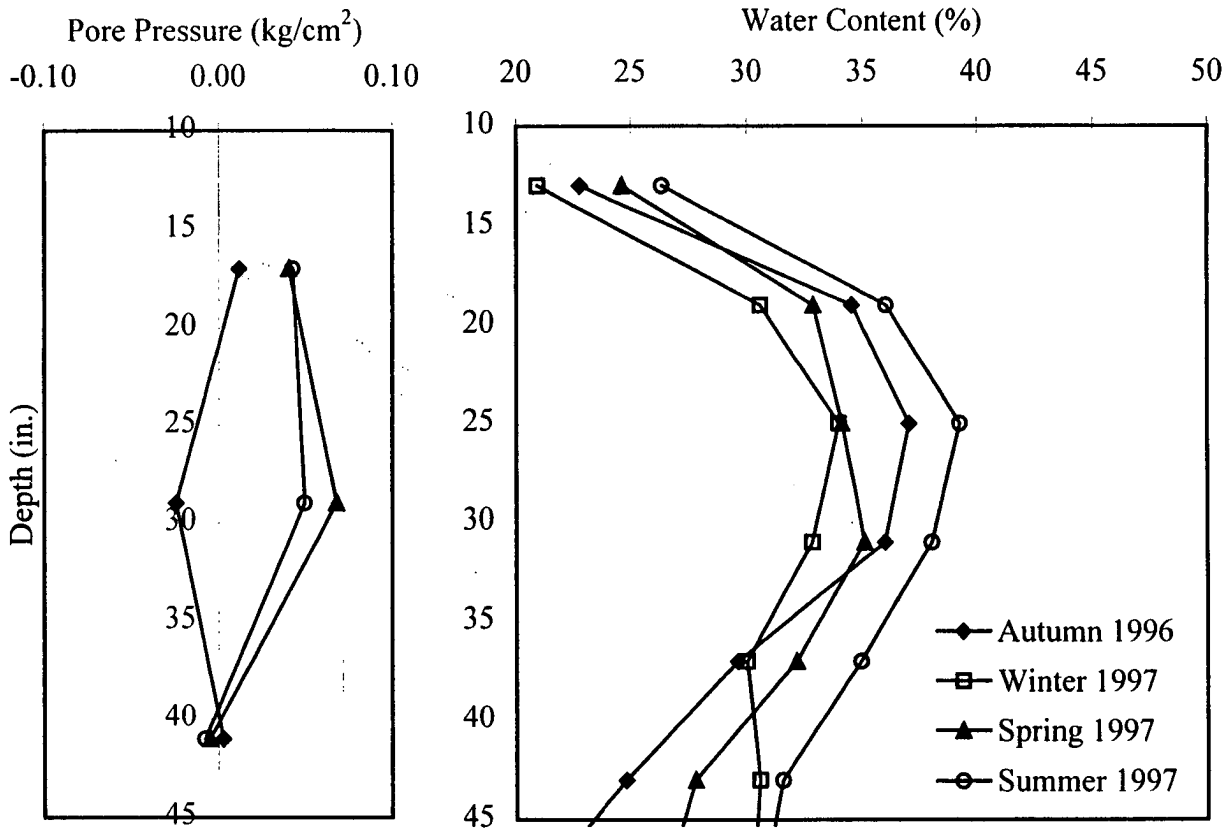

Figure 4.9. Pore Water Pressure and Water Content Measurements at SPS-2 S-4. Section 390263.

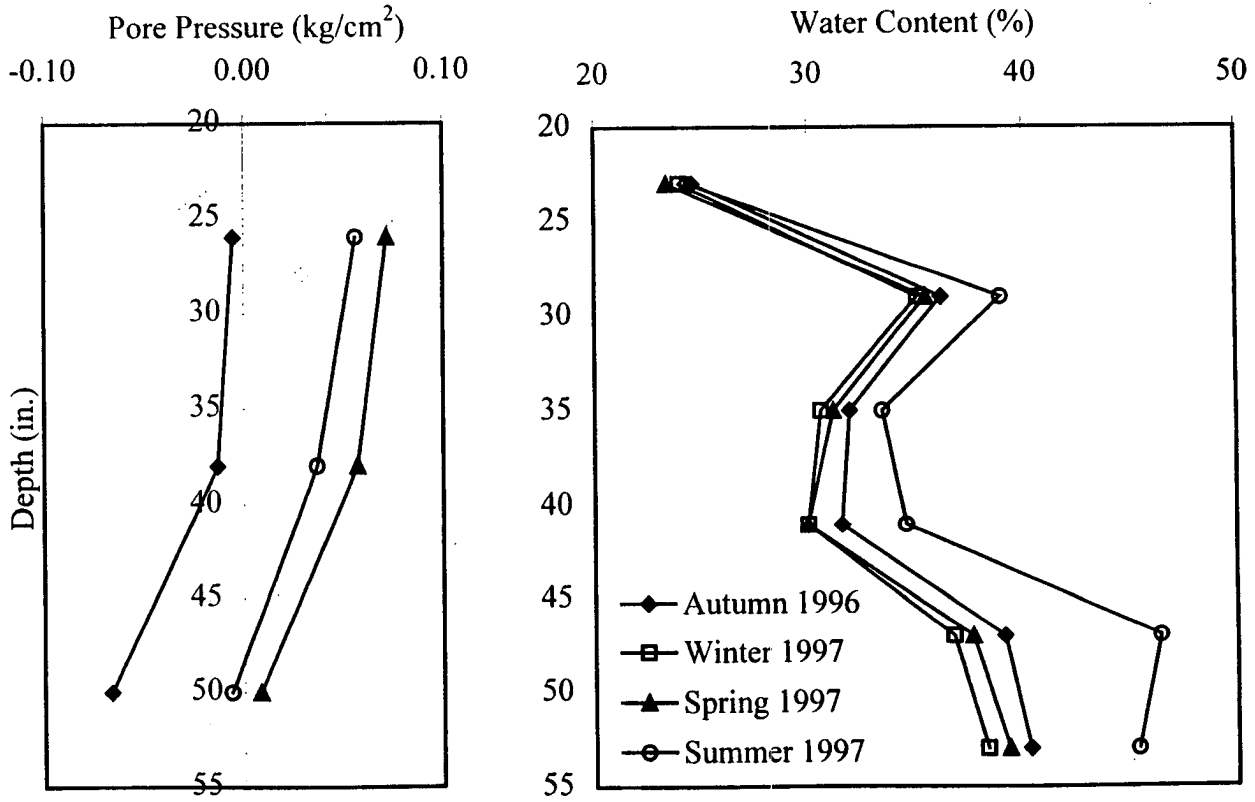

Figure 4.10. Pore Water Pressure and Water Content Measurements at SPS-9 SHRP. Section 390904.

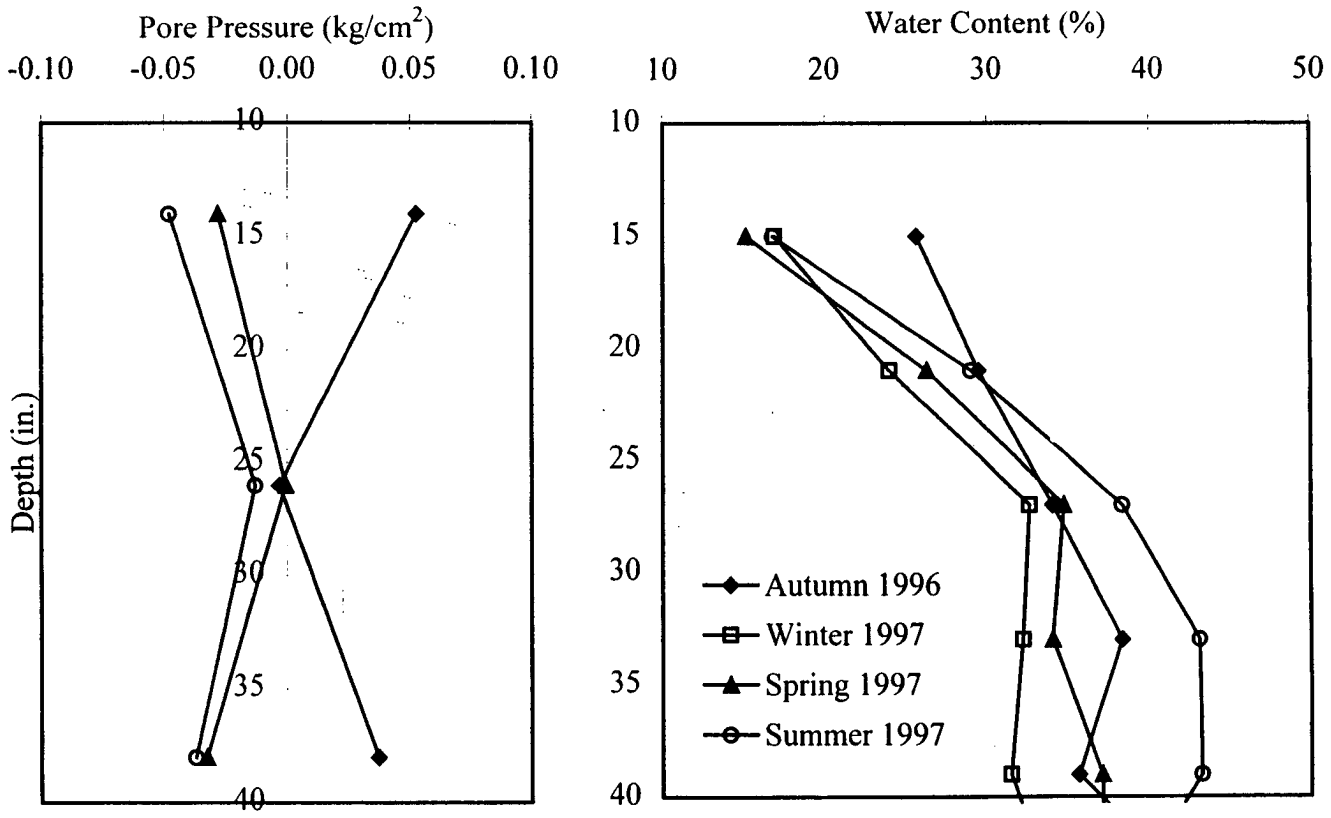

Figure 4.11. Pore Water Pressure and Water Content Measurements at SPS-2 J-11. Section 390211.

4.2 Laboratory Tests

4.2.1 Granular Material (Item 304)

4.2.1a Grain Size Tests

The particle size distributions obtained for the samples of the 304 aggregate are presented in Table 4.1. The values presented in the table are for percent, by weight, finer than the sieve size shown. The grain size data are also plotted for the nine 304 samples in Figure 4.12. It is clear from this figure that the samples were all similar in grain size distribution. All the samples were classified as well graded gravels with little fines.

4.2.1b Permeability Tests

The measured coefficient of permeability for each sample tested is presented in Table 4.2. As can be seen from the data presented, the permeability data are fairly high and range only between 2.0×10^{-2} cm/sec and 2.9×10^{-2} cm/second, reflecting the similarity observed in the grain size distributions.

Sample ID	Station	Sieve Size (mm)									
		51.	25.	19.	9.5	6.4	4.75	2.36	0.84	0.43	0.15
390204 – BG19	275+00	100	92.0	82.8	55.8	43.4	36.0	25.2	15.4	11.5	5.2
390901 – BG05	284+00	100	92.1	84.1	59.7	47.5	40.0	28.4	18.4	14.6	10.9
390210 – BG20	303+08	100	93.9	84.2	62.5	50.8	42.9	29.1	16.6	12.2	7.7
390902 – BG06	304+50	100	92.2	85.0	67.0	57.5	50.4	36.7	22.6	16.7	11.4
390101 – BG16	349+50	100	85.4	68.6	45.6	35.2	29.1	19.7	11.9	9.0	6.0
390209 – BG22	349+75	100	89.8	82.2	57.4	45.0	37.4	24.6	14.2	10.3	5.6
390102 – BG18	369+50	100	87.7	77.1	55.8	44.9	37.5	25.4	15.4	11.5	7.2
390203 – BG23	389+25	100	95.0	86.4	65.6	55.0	46.8	33.9	22.2	17.6	12.9
390108 – BG19	394+25	100	94.4	82.2	59.4	48.0	40.5	28.4	18.1	14.0	10.2

Table 4.1 Grain Size Distribution for the Granular Material (Item 304)

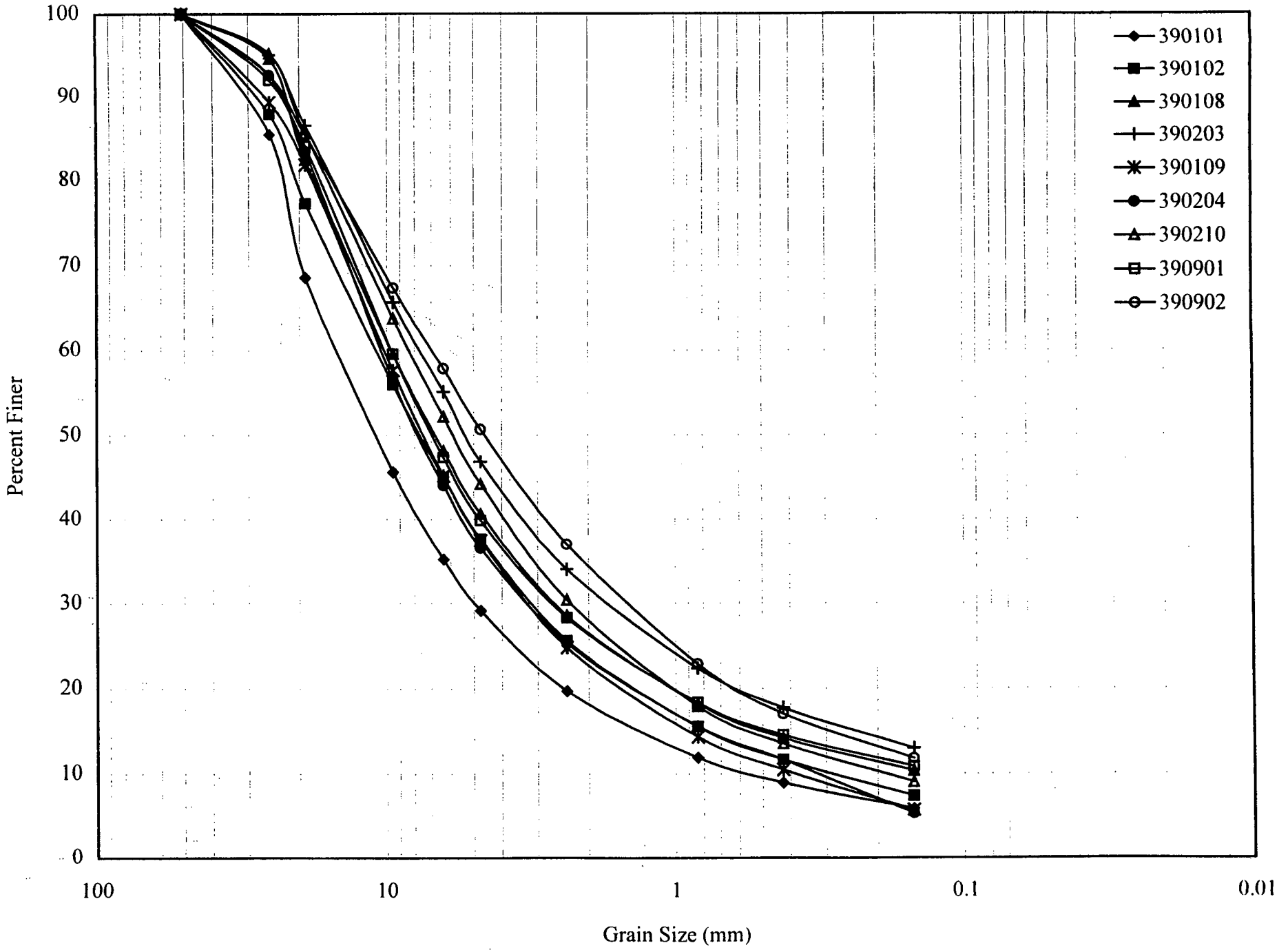

Figure 4.12. Grain Size Curves for Item 304 Samples

Sample ID	Station	Permeability (cm/sec)
390204 - BG19	275+00	$2.86x10^{-02}$
390210 - BG20	303+08	$2.15x10^{-02}$
390902 - BG06	304+50	$2.49x10^{-02}$
390101 - BG16	349+50	$2.46x10^{-02}$
390209 - BG22	349+75	$2.62x10^{-02}$
390102 - BG18	369+50	$2.33x10^{-02}$
390901 - BG05	384+00	$1.98x10^{-02}$
390203 - BG23	389+25	$2.01x10^{-02}$
390108 - BG19	394+25	$2.24x10^{-02}$

Table 4.2 Permeability Coefficients for the Granular Material (Item 304)

4.2.2 Cohesive Material

4.2.2a Atterberg Limits

The cohesive samples were found to be of a low to medium plasticity clay with liquid limit ranging between 29 and 40 and a plasticity index between 12 and 20.

4.2.2b Permeability Tests

The results of the falling head permeability tests conducted on the recompacted samples contained within the modified 10 cm I.D. compaction molds are presented in Table 4.3. The results of the permeability tests conducted on the undisturbed samples collected in the thin-walled (Shelby) tubes are also presented in Table 4.3.

Sample ID	Classification	Location	Permeability (cm/sec)
390204 - BG10 - Emb	CL (A-6)	281+00	$1.19x10^{-07}$
390901 - BG03 - Emb	CL (A-7-6)	378+00	$9.61x10^{-08}$
390101 - TS35 - A9	CL (A-6)	Section 390101	$4.12x10^{-08}$
390109 - TS18 - A18	CL (A-6)	Section 390109	$1.26x10^{-07}$
390112 - TS06 - A3	CL (A-6)	Section 390112	$1.76x10^{-07}$
390201 - TS22 - A15	CL (A-6)	Section 390201	$4.86x10^{-08}$
390203 - TS29 - A19	CL (A-6)	Section 390203	$1.87x10^{-07}$
390204 - TS16 - A2	CL (A-6)	Section 390204	$9.17x10^{-07}$
390260 - TS12 - A9-2	CL (A-6)	Section 390260	$6.00x10^{-08}$
390810 - TS04 - A8	CL (A-6)	Section 390810	$3.83x10^{-06}$
390902 - TS09 - A5	CL (A-6)	Section 390902	$3.23x10^{-07}$

Table 4.3 Permeability Coefficients for the Fine Grained Material

5 CONCLUSIONS AND RECOMMENDATIONS

5.1 Conclusions

Environmental instrumentation to measure temperature, soil moisture, frost depth and matric suction, was purchased, constructed, calibrated and installed at selected SPS sections. The tensiometers, which measured matric suction, showed that pore pressures have increased with time in the soils beneath the pavement. This increase in pore pressure occurred while the TDR probes were measuring a corresponding increase in soil moisture content.

Research demonstrates that unsaturated soil behaves differently from saturated soil, thus requiring different methods for determining actual strengths and compressibilities. A complete description of the stress regime requires an accurate measure of negative pore pressure, or matric suction. In a material that can sustain large negative pore pressures, water beneath the surface will be drawn into the profile, causing an overall decrease in the strength and an increase in compressibility that would result in increased deflections and possibly even soil failure. These increases in water content could be aggravated by pumping action due to repeated loads or be the result of poor drainage beneath and on either side of the pavement.

Loss of shear strength in the subgrade soils will greatly affect the performance of the pavement. As seasonal conditions change at the site, the degree of saturation in the subgrade soils would be expected to fluctuate. The first resistivity data were collected in late summer 1996. Naturally, they did not indicate frost at any depth and therefore the vertical flow of water would have been unimpeded. Later in the year as the temperatures at the site decreased below freezing for a sufficient amount of time, the near surface porewater froze and, over the winter months, the frost depth increased. In late winter 1997, the depth of frost penetration reached a maximum of about 0.8 to 1.0 meters. In the spring, as air temperatures increased, the upper portions of the frozen soils and base began to thaw. This resulted in lenses of frozen soils below soil that had thawed and vertical drainage would have been impeded. In this situation the thawed material would become excessively wet and pore pressures would be expected to increase locally. Under these conditions the negative pore water pressures which had existed above the water table would tend toward zero and the soil would lose that portion of the strength contributed by matric suction. At different locations both vertically and laterally the soil might posses little or no strength to support the soil or the pavement above it. If the support of the soil is reduced, increased pavement strains would result. This would, in turn, increase the effects of the traffic flow on the pavement and potentially cause premature failure.

As the soils thaw completely and precipitation decreases towards the end of summer and early fall, the water table may fall and the degree of saturation in the soil

may decrease. At this point, the strength of the soil will increase due to the contribution of matric suction to the effective confinement.

Readings from the weather station indicate that at a depth of 30.5 cm the soil suction was 50 kN/m^2 (0.5 bar) at the time of reading. The suction value at a depth of 61 cm was measured at 90 kN/m^2. These data indicate that the soil at 30.5 cm was at a higher degree of saturation than the soil at 61 cm. Conditions at the site indicated that precipitation had fallen the previous night, which would explain the readings from these tensiometers. The readings also indicate that the tensiometers do work properly when the tube is free of air and the tip is saturated. These conditions were insured during the installation of these probes and maintained by immediately filling the tubes with water and sealing.

5.2 Recommendations

Because of the strong tendency of the base and subgrade materials to support negative pore pressures initially unsaturated soils fairly quickly became saturated, thereby reducing apparent strength and stiffness properties. Additional monitoring of the pavement profiles is justified since the data collected to date indicate the drains have not prevented the base from becoming saturated. In future work it is recommended that ground water monitoring wells be installed at SPS sections containing tensiometers to allow for better interpretation of the readings. Further, new techniques for ensuring that the porous ceramic tips of the tensiometers installed are saturated for reliable readings should be investigated.

In addition it is suggested that the subgrade materials at each section instrumented with tensiometers be tested to determine the magnitude of negative pore pressure required for those materials to drain freely. At high values of negative pore pressure, the soil strength is greater and compressibility is lower than when the pore pressure is zero or positive. In the case of roadway design, considerable error could be introduced into an analysis if the soil properties are evaluated when the material is unsaturated unless the material is prevented from becoming saturated over time.

6 IMPLEMENTATION

We have shown that tensiometers can be used in conjunction with other instrumentation to establish the appropriate material properties required to analyze the performance of pavement sections. Installation of tensiometers and a study of the water pressures recorded will improve our understanding of how drains work.

7 REFERENCES

1. Sargand, S., *Development of an Instrumentation Plan for the Ohio SPS Test Pavement (DEL-23-17.48), Final Report,* Report No. FHWA/OH-94/019, October, 1994.
2. Rada, G.R., Elkins, G.E., Henderson, B. and Van Sambeek, R.J., *LTPP Seasonal Monitoring Program: Instrumentation Installation and Data Collection Guidelines, Version 2.1,* April, 1994.
3. Informational Brochure for 600 Series Porous Ceramics, Soilmoisture Equipment Corp., July, 1992.
4. Coduto, Donald P., *Foundation Design: Principles and Practices*, Prentice Hall, Englewood Cliffs, N.J., 1994.
5. Fredlund, D.G. and Rahardjo, H., *Soil Mechanics for Unsaturated Soils*, John Wiley and Sons, Inc., 1993
6. Rendulic, L., "Relation Between Void Ratio and Effective Principal Stresses For a Remolded Silty Clay," in *Proc. 1st Int. Conf. Soil Mech. Found. Eng.* (Cambridge, MA), vol. 3, 1936, pp. 48-51.
7. Skempton, W., "Effective Stress in Soils, Concrete and Rocks," in *Proc. Conf. Pore Pressure.* London: Butterworths, 1961, 4-16.
8. Terzaghi, K., "The Shear Resistance of Saturated Soils," in *Proc. 1st Int. Conf. Soil Mechanics and Foundation Engineering*, Cambridge, MA, Vol. 1, 1936, pp. 54-56.
9. Fredlund, D.G., "Soil Mechanics Principles that Embrace Unsaturated Soils," *Proc 11th Int. Conf. Soil Mech. Found. Eng.*, San Francisco, Vol. 2, 1985, pp. 465-473.
10. Fredlund, D.G. and Morgenstern, N.R., "Stress State Variables for Unsaturated Soils," *Journal of the Geotechnical Engineering Division*, ASCE, Vol. 13, GT5, May 1977, pp. 447-466.
11. Fredlund, D.G., Morgenstern, N.R. and Widger, R.A., "The Shear Strength of Unsaturated Soils," *Canadian Geotechnical Journal*, vol. 15, 1978, pp. 313-321.